Journal Name

COMMUNICATION

Stabilizing Hybrid Perovskites Against Moisture and Temperature via Non-Hydrolytic Atomic Layer Deposited Overlayers

Received 00th January 20xx,
Accepted 00th January 20xx

DOI: 10.1039/x0xx00000x

www.rsc.org/

In Soo Kim,[a,b] Alex B. F. Martinson*[a,b]

A novel non-hydrolytic (*nh*) surface chemistry is utilized to allow the direct synthesis of pinhole-fee oxide overlayers directly on conventional hybrid perovskite halide absorbers without damage. Utilizing water-free ALD Al_2O_3 passivation, a minimum of ten-fold increase in stability against relative humidity (RH) 85% was achieved along with a dramatically improved thermal resistance (up to 250 °C). Moreover, we extend this approach to synthesize *nh*-TiO_2 directly on hybrid perovskites to establish its potential in inverted photovoltaic devices as a dual stabilizing and electron accepting layer, as evidenced by photoluminescence (PL) quenching.

Organic-inorganic hybrid perovskite halides have now proven their merit as high performance light absorbers due to their tunable gap, exceptional optoelectronic properties and simple processing.[1-7] While still in its infancy, hybrid perovskite-based photovoltaics outperform a number of mature photovoltaic technologies in a lab setting with certified power conversion efficiencies as high as 20.1 %.[8]

However, a significant challenge to the practical application of most hybrid perovskites remains. Specifically, the presence of hygroscopic ionic small molecules - alkylammonium cations - has been identified as a primary source of the absorber's notorious sensitivity towards moisture and temperatures above 150 °C.[9-13] $CH_3NH_3PbI_3$ ($MAPbI_3$), for instance, rapidly degrades upon exposure to modest relative humidity at room temperature via:

$$CH_3NH_3PbI_3\ (s) \rightarrow PbI_2\ (s) + CH_3NH_3I\ (aq)$$

A related, but distinct, decomposition pathway is induced by heating above 150 °C even under an inert and dry environment, where methylamine[14] and hydroiodic acid[15] exist in the gas phase:

$$CH_3NH_3PbI_3\ (s) \rightarrow PbI_2\ (s) + CH_3NH_2 \uparrow + HI \uparrow$$

Various attempts have been made to improve system stability – modification of organic cation or halide chemistry,[16-18] two dimensional (2D) hybrid perovskites,[19] and macroscopic encapsulation.[20] While these measures may impede degradation processes the effect is often modest, transient, and adds device complexity. Synthetically-compatible, pinhole-free functional overlayers, in contrast, provide a simple route to surface chemical passivation as well as a physical barrier to diffusion in or out of the absorber. As such, integral/functional overlayers are expected to improve long-term stability as well as improve subsequent processing compatibility (e.g. processing environment, chemical compatibility) of hybrid perovskite-based devices for a wide range of applications.

Atomic layer deposition (ALD) is a chemically diverse vapour-phase deposition technique with the capability to synthesize ultra-thin and pinhole-free films with well-defined surface chemical control and precise physical thickness.[21-23] The vast majority of oxide ALD processes[24] invoke water (H_2O), hydrogen peroxide (H_2O_2) or ozone (O_3) as oxygen sources, often at temperatures equal to or greater than 150 °C. Unfortunately, these chemicals and temperatures are predicted to be in direct conflict with most hybrid perovskite halides and therefore appear to preclude the integrated overlayer approach. However, in this communication, we employ *low temperature non-hydrolytic* (i.e. waterless) ALD to establish stabilizing overlayers of Al_2O_3 or TiO_2 directly on $CH_3NH_3PbI_{3-x}Cl_x$ ($MAPbI_{3-x}Cl_x$) films. We demonstrate not only that oxide ALD conditions exist that are compatible with hybrid perovskite halides, but that the resulting systems exhibit dramatically improved stability against moisture (85% RH) and enhanced resistance to considerably higher temperatures (250 °C). We further demonstrate the capability of *nh*-TiO_2 to serve a dual role – stabilizing the absorber underlayer and accepting electrons in future inverted photovoltaic devices. Moisture and thermal stability of non-hydrolytic Al_2O_3 (*nh*-Al_2O_3) passivated films are examined both in realistic and accelerated environments using X-ray diffraction (XRD) and spectroscopic techniques.

Mixed perovskite halide, $CH_3NH_3PbI_{3-x}Cl_x$ ($MAPbI_{3-x}Cl_x$), films were spin-coated on glass substrates by one step process in a nitrogen (N_2) filled glove box as reported previously.[18, 25] Briefly, a 1:3 molar ratio of $PbCl_2$ and CH_3NH_3I (MAI) mixture was dissolved in

[a] *Materials Science Division, Argonne National Laboratory, 9700 S. Cass. Ave., Argonne, Illinois 60439, United States*
[b] *Argonne Northwestern Solar Energy Research (ANSER) Center, 2145 Sheridan Road, Evanston, IL 60208, United States*
*E-mail: martinson@anl.gov (Alex B. F. Martinson)
Electronic Supplementary Information (ESI) available. See
DOI: 10.1039/x0xx00000x

anhydrous N,N-dimethylformamide (DMF). The solution was then spin coated onto glass substrates followed by annealing at 100 °C for 1 h. A representative optical image of an as-deposited $MAPbI_{3-x}Cl_x$ is depicted in Fig. 1a. The samples indicate single phase $MAPbI_{3-x}Cl_x$ in absence of perovskite halides of the form $CH_3NH_3PbI_2Cl$, $CH_3NH_3PbICl_2$ or more importantly, PbI_2 in agreement with previous reports (Fig. 1e).[9, 12]

Al_2O_3 was chosen as a model overlayer material, owing to its good barrier properties[26, 27] and precedence for thin film passivation.[28, 29] At least 21 distinct ALD processes are known for Al_2O_3,[24] the most common of which involves reaction of trimethylaluminum (TMA) with either ozone (O_3) or water (H_2O). Although TMA is exceedingly reactive,[30-32] we speculated that the oxidants would be most detrimental to the halide perovskite. Therefore, we first examined the stability of $MAPbI_{3-x}Cl_x$ films at modest temperature under vacuum and under additional exposure to common ALD oxygen sources. As-deposited $MAPbI_{3-x}Cl_x$ films were exposed to O_3 and H_2O (half ALD cycles only) in an ALD reactor at 100 °C. The amount of precursor delivered into the chamber was chosen to reflect realistic Al_2O_3 synthetic conditions, 100 x 0.015 sec exposures for H_2O and 100 x 0.75 sec exposures for O_3. Exposure to O_3 quickly induces visible degradation of mixed halide hybrid perovskites to PbI_2 (yellow), Fig. 1b. XRD analysis reveals a nearly complete decomposition to PbI_2 and loss of all $MAPbI_{3-x}Cl_x$ crystallinity (Fig. 1e). While H_2O triggers a similar effect, changes in the optical constants are more subtle, suggesting only partial degradation. Indeed, a significant formation of PbI_2 was observed, yet some $MAPbI_{3-x}Cl_x$ crystallinity is retained under the brief and low-partial pressure exposure as verified by XRD (Fig. 1e). The effects of full ALD cycles (metal and oxygen sources) on $MAPbI_{3-x}Cl_x$ films was also investigated to probe the extent to which metal/ligand half cycles may protect against subsequent exposures to O_3 or H_2O. As illustrated in Fig. 1b, samples exposed to TMA/O_3 appear equally degraded by the naked eye. However, a closer look at the XRD data reveals an even more complete loss of film crystallinity (see also Fig. S1, ESI†). An analogous effect was observed with TMA/H_2O and $TTIP/H_2O$ (TiO_2), Fig. 1c. In contrast to the samples exposed to H_2O alone, visible changes became more apparent, implying an accelerated process of degradation, perhaps attributed to local heating due to the strongly exothermic reactions that result from full ALD cycles of TMA and H_2O.[33, 34] We note that the ALD of Al_2O_3 directly on hybrid perovskite halides using TMA and O_3 have recently been reported, however, the formation of PbI_2 is evident after a single full ALD cycle.[35]

In an attempt to avoid O_3- or H_2O-induced degradation, we developed a novel *non-hydrolytic* (*nh*) Al_2O_3 ALD process that is analogous to a previous report of *nh*-TiO_2 growth.[36, 37] We substitute aluminum triisopropoxide (AIP) for titanium tetraisopropoxide, but retain acetic acid (AA) as the source oxygen. At 100 °C the controlled growth of Al_2O_3 occurs a rate of ~0.1 Å/cycle (Fig. S2, ESI†, full ALD variable space analysis will be published elsewhere). We observe that $MAPbI_{3-x}Cl_x$ films exhibit remarkable resistance to at least 200 x 0.015 sec exposures of acetic acid (Fig. 1d) at 100 °C. The halide perovskite remains single phase without visible transformation or measurable loss of crystallinity as revealed by XRD (Fig. 1e). Building on this observation, we performed *nh*-ALD full cycles with AIP/AA (Al_2O_3) and TTIP/AA (TiO_2) on as-deposited $MAPbI_{3-x}Cl_x$ films. Again, we observe no significant optical change that might reveal absorber degradation (Fig. 1d). A careful analysis of the XRD data reveal complete suppression of PbI_2 formation without loss of hybrid perovskite halide crystallinity (Fig. 1e). There, in contrast to the archetypal Al_2O_3 ALD processes (e.g. TMA/O_3, TMA/H_2O), *nh*-ALD provides an effective route to depositing oxide overlayers directly on mixed halide hybrid perovskites without damaging this sensitive underlayer.

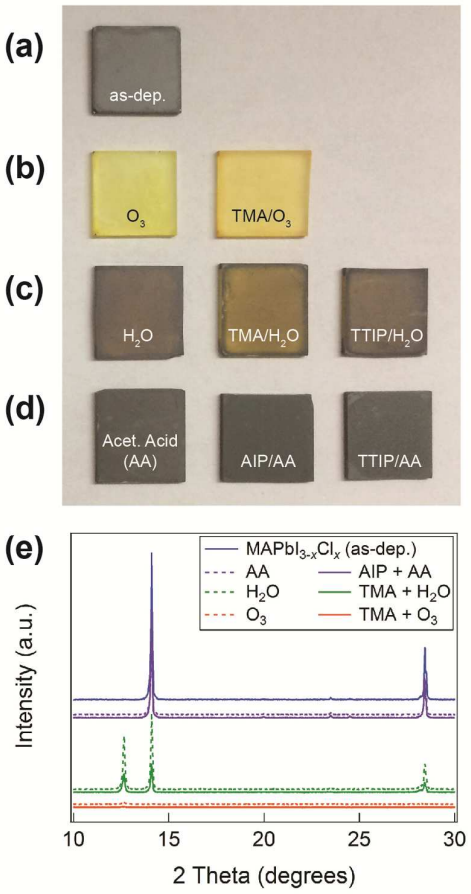

Fig. 1 (a) Optical image of representative as-deposited $MAPbI_{3-x}Cl_x$ thin film. (b), (c), and (d) $MAPbI_{3-x}Cl_x$ films exposed to O_3, H_2O, and acetic acid (AA), respectively. (e) XRD spectra of corresponding films.

The stabilizing effect of Al_2O_3 overlayers was investigated as a function of thickness with three sets of samples: unpassivated $MAPbI_{3-x}Cl_x$, 3 nm *nh*-Al_2O_3/$MAPbI_{3-x}Cl_x$, and 18 nm *hb*-Al_2O_3/$MAPbI_{3-x}Cl_x$ (Table 1). As *nh*-Al_2O_3 is a relatively slow ALD process (~0.1 Å/cycle), we employ a hybrid ALD (*hb*-ALD) process that utilizes both *nh*-ALD and subsequent TMA/H_2O ALD to deposit an additional 15 nm of Al_2O_3. This approach allows for more rapid barrier layer growth without damage to the hybrid perovskite underlayer (ESI†). Subsequently, 5 µL of water was drop-cast onto the three samples (Video S3, ESI†). The still images in Fig. 2 clearly reveal the extent to which the $MAPbI_{3-x}Cl_x$ degraded after each sample is allowed 2 minutes in contact with liquid water. As expected, the unpassivated $MAPbI_{3-x}Cl_x$ film degrades instantaneously upon contact with water.

Table 2 Performance of Al_2O_3 passivation on $MAPbI_{3-x}Cl_x$ as a function of thickness

Sample	Al_2O_3 ALD	Schematic Stack (drawn to scale)	Al_2O_3 Thickness (nm)	Stability of $MAPbI_{3-x}Cl_x$		
				5 µL H_2O (s)	RH 85 % (h)	250 °C (min)
A	N/A	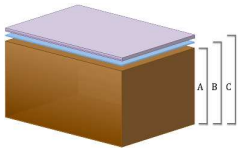	0	≈ 0	< 12	0.5
B	*nh*-ALD		3	< 1	~ 24	1
C	*hb*-ALD		18	> 900	> 210	> 30

Although slightly slowed, the 3 nm *nh*-Al_2O_3 passivated film still breaks down with seconds. The 18 nm *hb*-Al_2O_3 passivated film, in contrast, reveals no signs of degradation for at least 15 minutes. The resistance of a perovskite halide stack to liquid water has previously only been reported for a much thicker (ca. 200 nm) polymer film that doubled as metal-like current collector.[38] The stack indicated no signs of visible degradation after exposure to a stream of running water for 15 seconds. Of course, the effects of a liquid water droplet are quite different from exposure to water vapour in the ambient and likely above and beyond the requirement for most applications. As such the effect of Al_2O_3 overlayers were also examined in a more relevant accelerated environment of 85% relative humidity (RH). As others have previously reported,[10, 39] we see unpassivated films visibly degrade under 85% RH at room temperature, revealing substantial decomposition in less than 12 hours (Fig. S4, ESI†). The 3 nm *nh*-Al_2O_3 and 18 nm *hb*-Al_2O_3 passivated films, however, remained stable for 24 and over 200 hours, respectively, demonstrating more than an order of magnitude improvement (18 nm *hb*-Al_2O_3) in moisture-resistance over the control. The visible assessment of film degradation was corroborated by XRD and UV-vis spectroscopy throughout the degradation process in 85% RH (Fig. S5, ESI†). While the 3 nm *nh*-Al_2O_3 passivated films eventually degrade upon prolonged exposure to RH 85%, the 18 nm *hb*-Al_2O_3 passivated films have yet to visibly degrade after 3 weeks. Even the best barriers will allow slow diffusion of small molecules including water. As such, it appears likely that these ALD overlayers also induce a level of surface chemical passivation that may lead to longer-term stability, especially if coupled with macroscopic device encapsulation. The extent of chemical interaction is currently under investigation in our lab.

A striking improvement in thermal stability of $MAPbI_{3-x}Cl_x$ films was also observed with ALD Al_2O_3 stabilizing overlayers. Samples from the same set (Table 1) were annealed on a hot plate at 250 °C in a N_2 filled glove box with H_2O and O_2 levels below 0.1 ppm (Video S6, ESI†). Upon heating, the unpassivated film begins visibly decomposing in ~30 seconds, whereas the decomposition of the 3 nm *nh*-Al_2O_3 passivated film initiates around 1 minute. Remarkably, the 18 nm *hb*-Al_2O_3 passivated films exhibited 60x increase in thermal stability, remaining stable for at least 30 minutes prior to developing local regions of degradation (Fig. 3). To verify the extent of degradation, Fourier transform infrared (FTIR) spectroscopy and XRD measurements were performed on pre- and post-annealed samples (Fig. S7 and S8, ESI†). As can be seen in the FTIR spectra, characteristic vibrational modes of the methylammonium ($CH_3CH_2^+$) ions in $MAPbI_{3-x}Cl_x$[40] disappear in unpassivated films upon heating, which is in agreement with the reported mechanism of thermal degradation.[12] In contrast to unpassivated films, passivated films retained $CH_3CH_2^+$ ions in the structure throughout the heating process. These results were further verified by XRD measurements (Fig. S8, ESI†) performed after 70 s at 250 °C. In agreement with the FTIR results, the unpassivated films exhibit XRD peaks that suggest

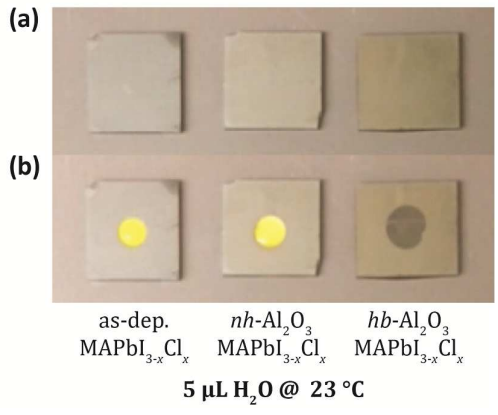

Fig. 2 Effect of 5 µL water droplet on $MAPbI_{3-x}Cl_x$ thin films as a function of time. a) and b) correspond to *t* = 0 s and 120 s, respectively.

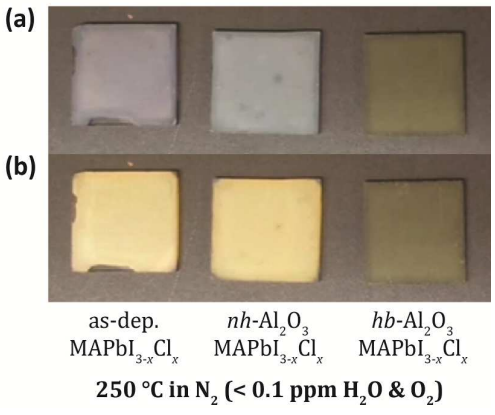

Fig. 3. Thermal stability of $MAPbI_{3-x}Cl_x$ thin films (*T* = 250 °C) as a function of time. a) and b) correspond to t = 0 s and 150 s, respectively.

complete decomposition into PbI_2, whereas the 3 nm *nh*-Al_2O_3 passivated films only showed partial degradation. Moreover, the 18 nm *hb*-Al_2O_3 remained as single phase $MAPbI_{3-x}Cl_x$ confirming exceptional endowed thermal stability even at 250 °C. Although the primary role that the Al_2O_3 overlayers play in the high temperature stabilization of $CH_3CH_2^+$ ions in $MAPbI_{3-x}Cl_x$ remains unclear, we speculate that surface chemical passivation may again play a role in addition to inhibited diffusion of CH_3NH_2 and HI out of $MAPbI_{3-x}Cl_x$. Further investigation is currently underway to understand these mechanisms.

Finally, we demonstrate the feasibility of utilizing *nh*-ALD for forming non-insulating overlayers with the potential to both stabilize the absorber and move charge, for example in photovoltaic applications with the well-known electron accepting material, TiO_2. Here, *nh*-TiO_2 was synthesized below or above $MAPbI_{3-x}Cl_x$ films to examine extent of photoluminescence (PL) – a marker for electron acceptor behaviour in this system. In both configurations, proximal *nh*-TiO_2 layers result in dramatic quenching of $MAPbI_{3-x}Cl_x$ PL, Fig. 4. These studies provide the first steps toward hybrid perovskite photovoltaics with a metal oxide electron acceptor in a stable inverted cell geometry.

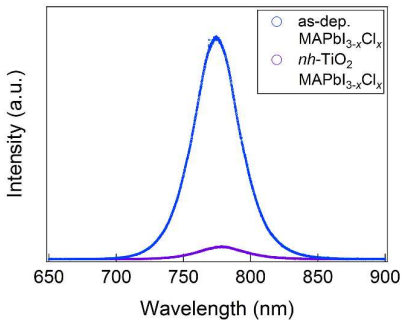

Fig. 4. Photoluminscence (PL) quenching of *nh*-TiO_2 / $MAPbI_{3-x}Cl_x$ films suggesting electronic communication with *nh*-TiO_2.

Conclusions

We have established a simple and effective approach to significantly improve the tolerance of hybrid perovskites to both moisture and temperature. A novel non-hydrolytic surface chemistry was introduced to grow ultrathin oxide barriers directly on hybrid perovskites without deposition-induced damage. Al_2O_3 passivated films reveal striking improvements in both moisture and thermal stability under accelerated aging environments, which we expect to provide enhanced durability in both future device use and device processing. *nh*-TiO_2 overlayers further reveal the potential for integrated optoelectronic device application, including hybrid perovskite-based photovoltaics.

Acknowledgements

This work was supported as part of the Argonne Northwestern Solar Energy Research Center, an Energy Frontier Research Center funded by the U.S. Department of Energy, Office of Science, Basic Energy Sciences under Award #DE-SC0001059. We thank Dr. T. R. Krause and Dr. M. S. Ferrandon for the use of their XRD. We also thank Dr. N. M. Markovic and Dr. P. Papa Lopes for the use of their PL system.

Notes and references

1 T. Baikie, Y. Fang, J. M. Kadro, M. Schreyer, F. Wei, S. G. Mhaisalkar, M. Graetzel and T. J. White, *J. Mater. Chem. A*, 2013, **1**, 5628-5641.
2 C. S. Ponseca, T. J. Savenije, M. Abdellah, K. Zheng, A. Yartsev, T. Pascher, T. Harlang, P. Chabera, T. Pullerits, A. Stepanov, J.-P. Wolf and V. Sundström, *J. Am. Chem. Soc.*, 2014, **136**, 5189-5192.
3 D. B. Mitzi, J. Chem. Soc., *Dalton Trans.*, 2001, 1-12.
4 C. C. Stoumpos, C. D. Malliakas and M. G. Kanatzidis, *Inorg. Chem.*, 2013, **52**, 9019-9038.
5 S. D. Stranks, G. E. Eperon, G. Grancini, C. Menelaou, M. J. P. Alcocer, T. Leijtens, L. M. Herz, A. Petrozza and H. J. Snaith, *Science*, 2013, **342**, 341-344.
6 G. Xing, N. Mathews, S. Sun, S. S. Lim, Y. M. Lam, M. Grätzel, S. Mhaisalkar and T. C. Sum, *Science*, 2013, **342**, 344-347.
7 C. Wehrenfennig, G. E. Eperon, M. B. Johnston, H. J. Snaith and L. M. Herz, *Advanced Materials*, 2014, **26**, 1584-1589.
8 NREL Record Cell Efficiencies. www.nrel.gov (accessed July 10, 2015).
9 A. Dualeh, N. Tétreault, T. Moehl, P. Gao, M. K. Nazeeruddin and M. Grätzel, *Adv. Funct. Mater.*, 2014, **24**, 3250-3258.
10 J. Yang, B. D. Siempelkamp, D. Liu and T. L. Kelly, *ACS Nano*, 2015, **9**, 1955-1963.
11 J. M. Frost, K. T. Butler, F. Brivio, C. H. Hendon, M. van Schilfgaarde and A. Walsh, *Nano Lett.*, 2014, **14**, 2584-2590.
12 A. Dualeh, P. Gao, S. I. Seok, M. K. Nazeeruddin and M. Grätzel, *Chem. Mater.*, 2014, **26**, 6160-6164.
13 B. Philippe, B.-W. Park, R. Lindblad, J. Oscarsson, S. Ahmadi, E. M. J. Johansson and H. Rensmo, *Chem. Mater.*, 2015, **27**, 1720-1731.
14 J. G. Aston, C. W. Siller and G. H. Messerly, *J. Am. Chem. Soc.*, 1937, **59**, 1743-1751.
15 W. F. Giauque and R. Wiebe, *J. Am. Chem. Soc.*, 1929, **51**, 1441-1449.
16 J. H. Noh, S. H. Im, J. H. Heo, T. N. Mandal and S. I. Seok, *Nano Lett.*, 2013, **13**, 1764-1769.
17 N. J. Jeon, J. H. Noh, W. S. Yang, Y. C. Kim, S. Ryu, J. Seo and S. I. Seok, *Nature*, 2015, **517**, 476-480.
18 J. M. Ball, M. M. Lee, A. Hey and H. J. Snaith, *Energ. Environ. Sci.*, 2013, **6**, 1739-1743.
19 I. C. Smith, E. T. Hoke, D. Solis-Ibarra, M. D. McGehee and H. I. Karunadasa, *Angew. Chem. Int. Ed.*, 2014, **53**, 11232-11235.
20 Y. Han, S. Meyer, Y. Dkhissi, K. Weber, J. M. Pringle, U. Bach, L. Spiccia and Y.-B. Cheng, *J. Mater. Chem. A*, 2015, **3**, 8139-8147.
21 S. M. George, *Chem. Rev.*, 2010, **110**, 111-131.
22 M. Leskelä and M. Ritala, *Thin Solid Films*, 2002, **409**, 138-146.
23 R. L. Puurunen, *J. Appl. Phys.*, 2005, **97**, 121301.
24 V. Miikkulainen, M. Leskelä, M. Ritala and R. L. Puurunen, *J. Appl. Phys.*, 2013, **113**, 021301.
25 M. M. Lee, J. Teuscher, T. Miyasaka, T. N. Murakami and H. J. Snaith, *Science*, 2012, **338**, 643-647.
26 E. Langereis, M. Creatore, S. B. S. Heil, M. C. M. van de Sanden and W. M. M. Kessels, *Appl. Phys. Lett.*, 2006, **89**, 081915.

27 M. D. Groner, S. M. George, R. S. McLean and P. F. Carcia, *Appl. Phys. Lett.*, 2006, **88**, 051907.
28 A. P. Ghosh, L. J. Gerenser, C. M. Jarman and J. E. Fornalik, *Appl. Phys. Lett.*, 2005, **86**, 223503.
29 D. H. Levy, D. Freeman, S. F. Nelson, P. J. Cowdery-Corvan and L. M. Irving, *Appl. Phys. Lett.*, 2008, **92**, 192101.
30 I. S. Kim, J. Borycz, A. E. Platero-Prats, S. Tussupbayev, T. C. Wang, O. K. Farha, J. T. Hupp, L. Gagliardi, K. W. Chapman, C. J. Cramer and A. B. F. Martinson, *Chem. Mater.*, 2015, DOI: 10.1021/acs.chemmater.5b01560.
31 C. L. Hinkle, A. M. Sonnet, E. M. Vogel, S. McDonnell, G. J. Hughes, M. Milojevic, B. Lee, F. S. Aguirre-Tostado, K. J. Choi, H. C. Kim, J. Kim and R. M. Wallace, *Appl. Phys. Lett.*, 2008, **92**, 071901.
32 M. Milojevic, F. S. Aguirre-Tostado, C. L. Hinkle, H. C. Kim, E. M. Vogel, J. Kim and R. M. Wallace, *Appl. Phys. Lett.*, 2008, **93**, 202902.
33 A. W. Ott, J. W. Klaus, J. M. Johnson and S. M. George, *Thin Solid Films*, 1997, **292**, 135-144.
34 Y.-S. Min, Y. J. Cho and C. S. Hwang, *Chem. Mater.*, 2005, **17**, 626-631.
35 X. Dong, X. Fang, M. Lv, B. Lin, S. Zhang, J. Ding and N. Yuan, *J. Mater. Chem. A*, 2015, **3**, 5360-5367.
36 E. Rauwel, G. Clavel, M.-G. Willinger, P. Rauwel and N. Pinna, *Angew. Chem. Int. Ed.*, 2008, **47**, 3592-3595.
37 G. Clavel, E. Rauwel, M.-G. Willinger and N. Pinna, *J. Mater. Chem.*, 2009, **19**, 454-462.
38 S. N. Habisreutinger, T. Leijtens, G. E. Eperon, S. D. Stranks, R. J. Nicholas and H. J. Snaith, *Nano Lett.*, 2014, **14**, 5561-5568.
39 J. Liu, S. Pathak, T. Stergiopoulos, T. Leijtens, K. Wojciechowski, S. Schumann, N. Kausch-Busies and H. J. Snaith, *J. Phys. Chem. Lett.*, 2015, **6**, 1666-1673.
40 N. Onoda-Yamamuro, T. Matsuo and H. Suga, *J. Phys. Chem. Solids*, 1990, **51**, 1383-1395.

Journal Name

COMMUNICATION

Broader Context

Organic-inorganic hybrid perovskites have emerged as one of the most promising materials classes for demanding optoelectronic applications that include photovoltaics, light emitting diodes, and photodetectors. For photovoltaic application in particular, an important prerequisite is the long-term stability against environmental moisture and temperature. Most hybrid perovskite materials are, however, prone to both moisture- and temperature-induced degradation, and will therefore require new and perhaps numerous stabilization strategies to retain their desirable properties. While atomic layer deposition (ALD) provides an efficient route to synthesizing pinhole-free barriers with chemical control, typical processes involving water as an oxygen source immediately trigger the decomposition process in hybrid perovskites. Here, we utilize a novel non-hydrolytic surface chemistry to synthesize ultrathin oxide barriers directly on hybrid perovskites without damage. This may open up opportunities to fabricate a wide range of optoelectronic devices with long-term stability.

Fig. S1. XRD spectra of $MAPbI_{3-x}Cl_x$ films exposed to O_3 (dark orange) and TMA/O_3 (orange).

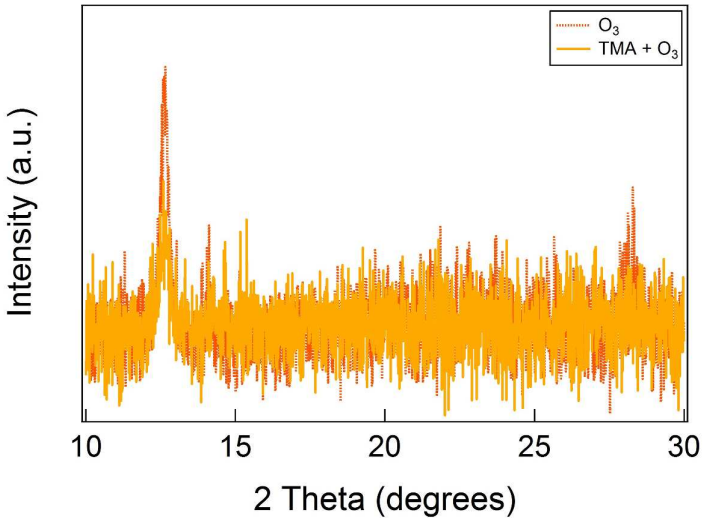

Fig. S2. In-situ quartz crystal microbalance (QCM) data recorded during 30 cycles of *nh*-Al_2O_3 ALD.

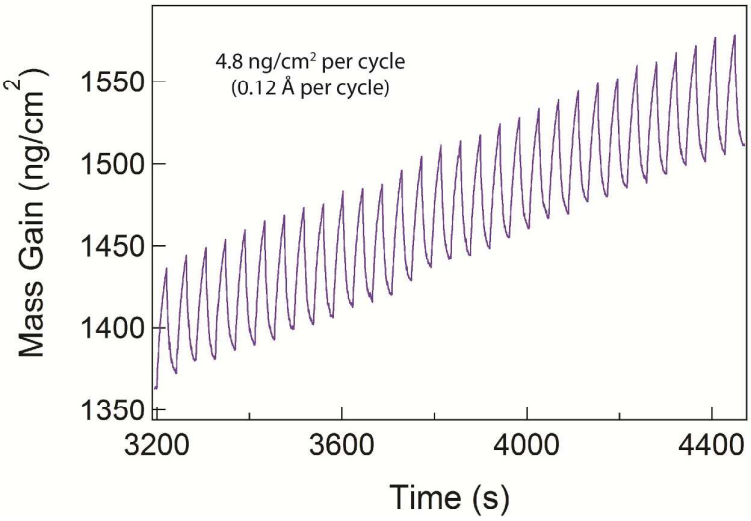

Video S3. Degradation of $MAPbI_{3-x}Cl_x$ films upon contact with 5 µL water droplet. Unpassivated, 3 nm *nh*-Al_2O_3, and 18 nm *hb*-Al_2O_3 (left to right).

VIDEO S3

Fig. S4. Degradation of $MAPbI_{3-x}Cl_x$ films in RH 85% as a function of time. Unpassivated, 3 nm *nh*-Al_2O_3, and 18 nm *hb*-Al_2O_3 (left to right). a), b), and c) correspond to t = 0, 6, and 48 h, respectively.

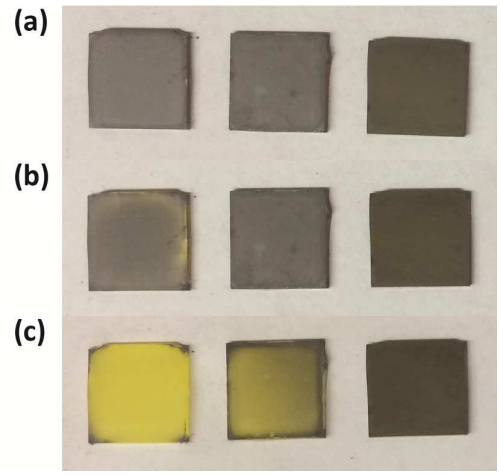

Fig. S5. UV-vis spectra of unpassivated $MAPbI_{3-x}Cl_x$ films in RH 85% as a function of time.

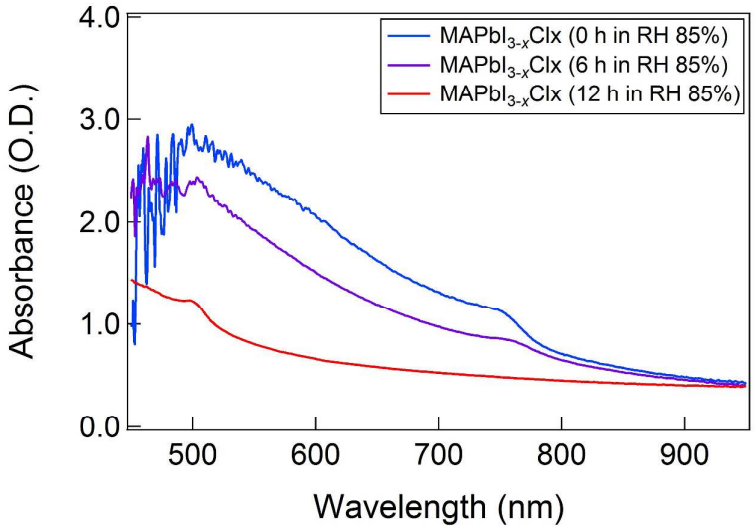

Video S6. Degradation of $MAPbI_{3-x}Cl_x$ films upon heating on a hotplate at 250 °C in N_2 filled glove box.

VIDEO S6

Fig. S7. FTIR spectra of unpassivated and 18 nm *hb*-Al_2O_3 passivated $MAPbI_{3-x}Cl_x$ films before and after annealing at 250 °C in a N_2 filled glove box.

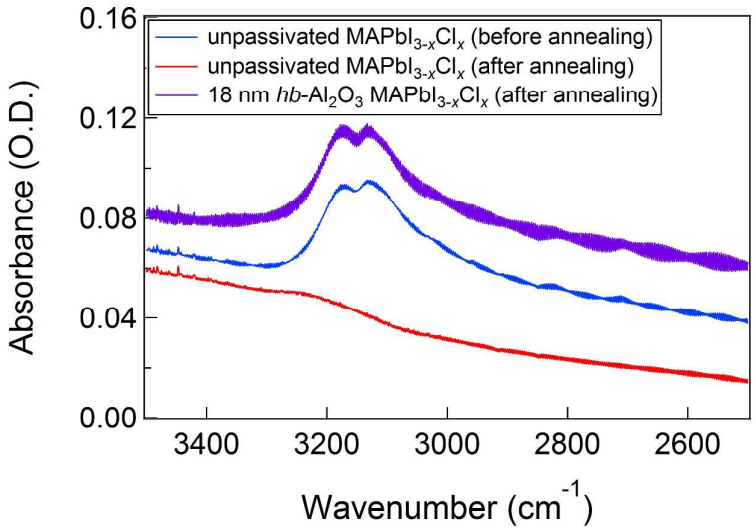

Fig. S8. XRD spectra of unpassivated, 3 nm *nh*-Al_2O_3, and 18 nm *hb*-Al_2O_3 passivated $MAPbI_{3-x}Cl_x$ films after annealing at 250 °C in N_2 filled glove box (t = 70 s).

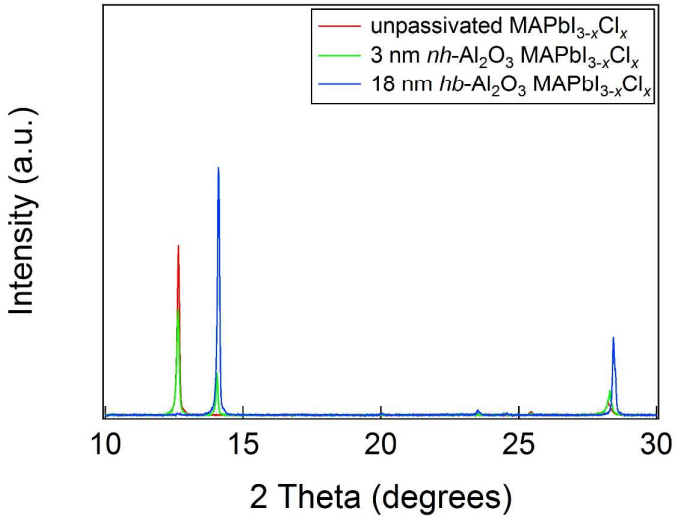

Table of Contents Graphic

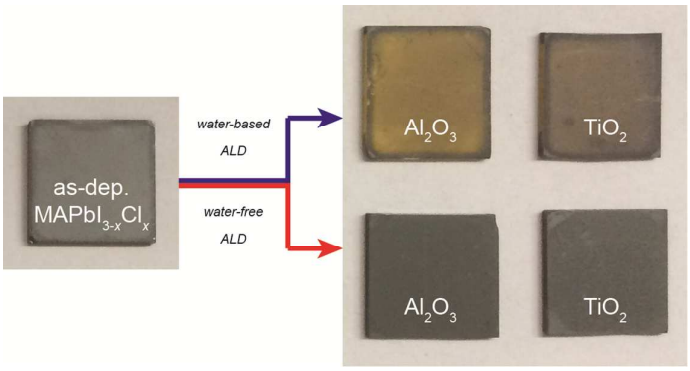

Non-hydrolytic atomic layer deposited oxide overlayers fabricated directly on perovskites results in improved stability against moisture and temperature.